HHS Public Access

Author manuscript

Brain Behav Immun. Author manuscript; available in PMC 2017 June 01.

Published in final edited form as:

Brain Behav Immun. 2017 March ; 61: 326–339. doi:10.1016/j.bbi.2016.12.012.

Pinocembrin protects hemorrhagic brain primarily by inhibiting toll-like receptor 4 and reducing M1 phenotype microglia

Xi Lan, **Xiaoning Han**, **Qian Li**, **Qiang Li**, **Yufeng Gao**, **Tian Cheng**, **Jieru Wan**, **Wei Zhu**, and **Jian Wang**[*]

Department of Anesthesiology and Critical Care Medicine, the Johns Hopkins University School of Medicine, Baltimore, MD 21205, USA

Abstract

Neuroinflammation is a major contributor to intracerebral hemorrhage (ICH) progression, but no drug is currently available to reduce this response and protect against ICH-induced injury. Recently, the natural product pinocembrin has been shown to ameliorate neuroinflammation and is undergoing a phase II clinical trial for ischemic stroke treatment. In this study, we examined the efficacy of pinocembrin in an ICH model, and further examined its effect on microglial activation and polarization. In vivo, pinocembrin dose-dependently reduced lesion volume by 47.5% and reduced neurologic deficits of mice at 72 h after collagenase-induced ICH. The optimal dose of pinocembrin (5 mg/kg) suppressed microglial activation as evidenced by decreases in CD68-positive microglia and reduced proinflammatory cytokines tumor necrosis factor (TNF)-α, interleukin (IL)-1β, and IL-6. Pinocembrin also reduced the number of classically activated M1-like microglia without affecting M2-like microglia in the perilesional region. Additionally, pinocembrin decreased the expression of toll-like receptor (TLR)4 and its downstream target proteins TRIF and MyD88. The protection by pinocembrin was lost in microglia-depleted mice and in $TLR4^{lps\text{-}del}$ mice, and pinocembrin failed to decrease the number of M1-like microglia in $TLR4^{lps\text{-}del}$ mice. In lipopolysaccharide-stimulated BV-2 cells or primary microglia, pinocembrin decreased M1-related cytokines and markers (IL-1β, IL-6, TNF-α, and iNOS), NF-κB activation, and TLR4 expression, but it did not interfere with TLR4/MyD88 and TLR4/TRIF interactions or affect microglial phagocytosis of red blood cells. Inhibition of the TLR4 signaling pathway and reduction in M1-like microglial polarization might be the major mechanism by which pinocembrin protects hemorrhagic brain. With anti-inflammatory properties, pinocembrin could be a promising new drug candidate for treating ICH and other acute brain injuries.

Keywords

Intracerebral hemorrhage; Pinocembrin; Microglial polarization; Toll-like receptor 4

[*]Corresponding author at: Department of Anesthesiology and Critical Care Medicine, Johns Hopkins University School of Medicine, 720 Rutland Ave, Ross Bldg 370B, Baltimore, MD 21205, USA. jwang79@jhmi.edu (J. Wang).

Potential conflicts of interest

Nothing to report.

1. Introduction

Intracerebral hemorrhage (ICH) is a significant cause of morbidity and mortality throughout the world (Morgenstern et al., 2010; Palacio and Hart, 2011). However, developing a targeted therapy or an effective drug to improve ICH outcomes remains a challenge. One potential target is the toll-like receptor (TLR) family. TLRs play an important role in the innate immune system (Avila and Gonzalez-Espinosa, 2011; Garcia-Bonilla et al., 2014), and TLR4 has been shown to be associated with ICH development (Kong and Le, 2011; Lively and Schlichter, 2012). It has been reported that elevated TLR4 is associated with poor outcomes of ICH (Fang et al., 2014; Rodriguez-Yanez et al., 2012; Yuan et al., 2015) and that TLR4 inhibition decreases secondary inflammatory damage after ICH (Wang et al., 2013b). Although it is known that lipopolysaccharide (LPS) is an exogenous ligand of TLR4, to date, no antagonist has shown success in clinic trials. Therefore, the feasibility of using TLR4 as a drug target for ICH needs further study.

In the brain's initial immune response of defense against ICH injury, microglia are rapidly activated and accumulate in the lesion site where they recruit other immune cells (Lan et al., 2011; Wang and Dore, 2007). However, the roles of activated microglia in ICH are still debated. Activated microglia/macrophages exhibit different phenotypes in different microenvironments and provide distinct functions (Boche et al., 2013; Zhang et al., 2016). In particular, M1-polarized microglia/macrophages are considered "classically activated" phenotypes that can increase proinflammatory cytokines and upregulate reactive oxygen and nitrogen species. In contrast, M2-polarized microglia/macrophages secrete anti-inflammatory cytokines and growth factors (Miron et al., 2013; Zhang et al., 2016), exerting the opposite effects of M1 microglia (Shechter and Schwartz, 2013). Studies have shown that in ischemic stroke, M2 microglia appear early in response to injury and later transition to an M1 phenotype (Hu et al., 2012; Perego et al., 2011). However, microglial polarization in ICH has not been well characterized.

Previous studies have shown that pinocembrin (5, 7-dihydroxyflavanone, Supplementary Fig. 1), a natural product extracted from propolis, is able to protect against cerebral ischemia by providing neuroprotection (Shi et al., 2011; Wu et al., 2013), decreasing oxidative stress (Liu et al., 2008), improving neurovascular unit function (Liu et al., 2008; Meng et al., 2011), and increasing expression of soluble epoxide hydrolase (Wang et al., 2013a). It also inhibits neuroinflammation by downregulating the receptor for advanced glycation end products (RAGE) and related downstream molecules (Liu et al., 2014, 2012). Importantly, pinocembrin is able to pass through the blood–brain barrier (BBB) by a passive transport process partly conducted by P-glycoprotein (Yang et al., 2012). Based on these data, the State Food and Drug Administration of China approved clinical trials of pinocembrin for ischemic stroke, and it is now in Phase II clinical trials (https://clinicaltrials.gov/ct2/show/NCT02059785).

Current data indicate that pinocembrin, which has been chemically synthesized (Lan et al., 2016), might be promising for ICH treatment. However, its efficacy in the ICH model remains to be determined because the pathogenesis of ICH is different from that of ischemic stroke. Moreover, the therapeutic target of pinocembrin is still unknown, its mechanisms of

action are unclear, and its effects on microglial activation and polarization must be ascertained. Here, we tested pinocembrin in a mouse model of ICH and found that it reduced inflammatory response in vivo and in vitro primarily by reducing TLR4 expression. In addition, we observed different microglial phenotypes in wild-type (WT) and TLR4$^{lps\text{-}del}$ mice subjected to ICH and showed how pinocembrin protects against ICH injury primarily by suppressing M1 microglial polarization via TLR4 inhibition, suggesting that it might be an effective drug to treat ICH.

2. Materials and methods

2.1. Animals

All animal experiments were conducted in accordance with guidelines from the National Institutes of Health and were approved by the Institutional Animal Care and Use Committee at Johns Hopkins University School of Medicine. Adult male WT C57BL/6 mice (8–10 weeks old) were purchased from Charles River Laboratories (Frederick, MD). TLR4$^{lps\text{-}del}$ male mice on C57BL/6 background were obtained from The Jackson Laboratory. CX3CR1$^{GFP/+}$ male mice on C57BL/6 background (8–10-week old) obtained from Dr. Jonathan Bromburg (University of Maryland, Baltimore, MD) were used for visualization of microglia.

2.2. ICH mouse model

After anesthetizing mice with 1–3% isoflurane and ventilating them with oxygen-enriched air (20%:80%) via a nose cone, we injected collagenase VII-S (0.075 U in 0.5 μl sterile saline, Sigma-Aldrich) into the striatum (0.1 μl/min) at the following coordinates relative to the bregma: 0.8 mm anterior, 2 mm lateral, and 2.8 mm deep (Chang et al., 2014; Zhao et al., 2015b). Core body temperature was maintained at 37.0 ± 0.5 °C throughout the surgery and recovery periods with a DC Temperature Controller 40-90-8D (FHC Inc. ME). Sham control mice received the same treatment, including needle insertion, but without collagenase injection.

2.3. Pinocembrin administration

Pinocembrin (purity > 99%), a kind gift from Dr. Guanhua Du (Institute of Materia Medica, Chinese Academy of Medical Sciences & Peking Union Medical College, Beijing, China), was dissolved in 20% hydroxypropyl-β-cyclodextrin (HP-β-CD, Sigma-Aldrich) as described previously (Lan et al., 2016; Liu et al., 2014). Animals were randomly assigned (http://www.randomizer.org/) to receive pinocembrin (2.5, 5, 10 mg/kg) or vehicle via tail vein (i.v.) at 2 h after ICH and then twice daily until euthanasia. The delivery route, dosing, and treatment regimens were based on previous work (Lan et al., 2016; Zhao et al., 2014) and our pilot studies. We divided animals into four groups: 1) Sham+vehicle: mice that were injected with saline intrastriatally plus i.v. injection of 20% HP-β-CD; 2) Sham+Pino: mice that were injected with saline intrastriatally plus i.v. injection of pinocembrin; 3) ICH +vehicle: mice that underwent ICH induction plus i.v. injection of 20% HP-β-CD; 4) ICH +Pino: mice that underwent ICH induction plus i.v. injection of pinocembrin. In another set of experiments, TLR4$^{lps\text{-}del}$ mice and WT mice underwent ICH induction and were treated with either pinocembrin (5 mg/kg) or 20% HP-β-CD. Subgroups of mice that were depleted

of microglia (Fernandez-Lopez et al., 2016) underwent ICH induction and were treated with either pinocembrin (5 mg/kg) or 20% HP-β-CD (Supplementary methods 1). Investigators blinded to the treatment groups evaluated outcomes in all mice and performed data analysis. All mice were included (n = 269), but those in which ICH induction failed or that died before the end of the study (n = 13) were excluded from the final data analysis.

2.4. Assessment of ICH outcome

2.4.1. Behavior experiments—Neurologic deficits of mice were evaluated by a 24-point scoring system, the wire hanging test, and the corner turn test on days 1 and 3 post-ICH (Cheng et al., 2016; Zhu et al., 2014). All behavior tests were performed in a blinded manner.

2.4.2. Lesion volume and hematoma size—At 3 days after ICH induction, brain lesion volume was assessed with Luxol fast blue staining as we previously described (Chang et al., 2014; Wu et al., 2012). At 3 or 5 days post-ICH, brains were cut into 1-mm sections, and we evaluated hematoma clearance by measuring hematoma size in the striatum (Wang et al., 2003).

2.4.3. Brain water content—At 3 days after ICH induction, brain water content was measured as a surrogate for brain edema. It was calculated as [(wet weight − dry weight)/wet weight] × 100% (Han et al., 2016).

2.5. Immunostaining

2.5.1. Immunostaining of brain tissue—Mouse brain was cut into 30-μm-thick coronal sections for immunostaining as described previously (Han et al., 2016). Sections were incubated overnight at 4 °C with primary antibodies to CD68 (rat anti-mouse, 1:200, AbD Serotec), Iba1 (rabbit, 1:500, Wako), CD16/32 (mouse, 1:100, BD Biosciences), YM-1 (rabbit, 1:200, Stemcell), YM-1 (rat, 1:200, R&D Systems), or TLR4 (mouse, 1:100, Abcam) and then for 90 min with Alexa Fluor 594 secondary antibody (goat anti-rabbit, goat anti-mouse, or goat anti-rat, 1:1000, Life Technologies). Sections were mounted with VECTA-SHIELD mounting medium (which contained DAPI for fluorescence) and examined under a Nikon Eclipse 90i fluorescence microscope. Omission of the primary antibody was used as a control.

An investigator blinded to treatment group analyzed the number of microglia and double-labeled cells in a defined region of interest in the striatum around the hematoma (Chang et al., 2014; Zhao et al., 2015b). Brain sections with similar lesion areas were selected. Cell counts and colocalization of $CD68^+$, $CD16/32^+$, $YM\text{-}1^+$/CX3CR1 (GFP) and $CD68^+$, $CD16/32^+$, $YM\text{-}1^+/Iba1^+$ were analyzed with ImageJ software (1.4, NIH). Positive cells from five optical fields at 20 × 10 magnification in each of the three sections per animal were averaged. Cell densities per square millimeter were calculated.

2.5.2. Immunostaining of primary microglia—$CX3CR1^{GFP/+}$ mouse primary microglia were fixed with 4% paraformaldehyde (PFA), blocked with 5% bovine serum albumin (BSA), and incubated with primary antibody to NF-κB p65 (1:400, CST) or TLR4

(1:100, Abcam) at 4 °C overnight. Microglia were then incubated at room temperature with appropriate secondary antibody (Alexa Fluor 594 goat anti-rabbit or goat anti-mouse, 1:1000, Life Technologies) for 1 h. Cell nucleus was stained with DAPI.

2.6. ELISA

Concentrations of proinflammatory cytokines (IL-1β, IL-6, and TNF-α) in brain tissue or cell culture medium were measured by ELISA (R&D System) (Chang et al., 2014; Wang et al., 2003).

2.7. Magnetic-activated cell sorting (MACS) and Western blot analysis

For microglial isolation, we dissociated brain tissue by MACS (Held-Feindt et al., 2010; Lee and Lufkin, 2012) using the Gentle-MACS Dissociator and Neural Tissue Dissociation kit (Miltenyi Biotec). Three coronal hemorrhagic or uninjured brain sections (4-mm thickness in total) were collected for microglial isolation. Single-cell suspensions were incubated with anti-myelin immunoglobulin-conjugated magnetic microbeads (Myelin Removal Kit; Miltenyi Biotec) to remove myelin. Cells were then incubated with CD11b MicroBeads at 4 °C for 15 min. After the cells were washed, cell supernatants were applied to LS columns for magnetic separation (Miltenyi Biotech). The isolated microglia were then lysed in RIPA buffer for Western blot analysis.

For Western blotting, we used antibodies to the following proteins: inducible nitric oxide synthase (iNOS, 1:1000, Cell Signaling), phospho-NF-κB-p65 (1:1000, Cell Signaling), phospho-IKKα/β (1:1000, Cell Signaling), IKKα (1:1000, Cell Signaling), IKKβ (1:1000, Cell Signaling), TLR4 (1:200, Santa Cruz), MyD88 (1:200, Santa Cruz), TRIF (1:500, GeneTex), YM-1 (1:500, Stemcell), β-actin (1:5000, Santa Cruz), and Histone 3 (H3, 1:200, Santa Cruz). Briefly, equal amounts of protein (50 μg) were separated by 4–20% SDS-PAGE and transferred onto polyvinylidene fluoride membranes. The membranes were blocked with 5% milk, incubated with primary antibodies at 4 °C overnight, and then incubated with peroxidase-coupled goat anti-rabbit or anti-mouse secondary antibody (1:5000; CST). Membranes were immersed in enhanced chemiluminescence (ECL) solution and exposed under an Image-Quant ECL Imager (GE Healthcare).

2.8. Cell culture and pinocembrin treatment

2.8.1. Mouse primary microglial culture—Newborn CX3CR1$^{GFP/+}$ mice were used to culture primary microglia as described previously (Bal-Price and Brown, 2001). Briefly, cortex-striatum was dissected from brain and cut into 1–3-mm^2 pieces. Cells were dissociated in D-Hanks' solution containing 0.25% trypsin (Quality Biological) and plated onto 75-cm^2 cell culture flasks at 1×10^7 cells/ml in Dulbecco's modified Eagle's medium/Ham's F-12 (DMEM/F12, Life Technologies) with 10% fetal bovine serum (FBS, Life Technologies). After 14 days, microglia were removed from mixed glial cells by shaking at 200 rpm at 37 °C for 4 h and then seeded into 24-well plates. Microglia that were >95% positive for CX3CR1$^+$ were used in experiments (Supplementary Fig. 2).

2.8.2. Microglial cell line culture—The murine microglial cell line BV-2 (Blasi et al., 1990; Bocchini et al., 1992) (a kind gift from Dr. Sujatha Kannan, Johns Hopkins University,

passage <30) was cultured in RPMI 1640 medium supplemented with 10% FBS, 1% penicillin/streptomycin (Quality Biological), and 2 mM L-glutamine (Quality Biological) at 37 °C and 5% CO_2.

2.8.3. Pinocembrin treatment—We found that pinocembrin at doses of 10 μM and below did not reduce cell viability (Supplementary Fig. 3A and B). Therefore, we pre-incubated microglia with 1, 3, or 10 μM pinocembrin for 1 h before stimulating them with LPS (50 ng/ml). After 30 min, we extracted nuclear and cytoplasmic proteins from BV-2 cells to measure NF-κB p65 translocation by Western blot, and used primary microglia to show NF-κB p65 translocation by immunostaining. After 24 h of LPS stimulation, we collected whole cell lysates to measure iNOS and TLR4; we used supernatants to detect the levels of proinflammatory cytokines and nitric oxide (NO).

2.9. Small interfering RNA (siRNA) transfection

At 60% confluence, BV-2 cells were transfected with 10 nM TLR4 siRNA (Origene) or universal scrambled negative control siRNA (Origene) by using Lipofectamine RNAiMAX (Life Technologies). At 48 h after transfection, cells were used for various experiments. (Supplementary Fig. 4)

2.10. Nitric oxide assay

The production of NO-derived nitrite was determined by the Griess reagent kit (BIO-RAD) as described previously (Drew and Chavis, 2001).

2.11. Immunoprecipitation

BV-2 cells were lysed in NP-40 buffer (Life Technologies) supplemented with protease inhibitor cocktail (Roche). Cell lysate was incubated with Dynabeads Protein G (Life Technologies) and TLR4 antibody (Santa Cruz). Immunoblotting was conducted to probe the resolved complexes with TLR4, MyD88 (Santa Cruz), and TRIF (Imgenex)

2.12. Statistical analysis

All data are presented as means ± S.D. Comparisons of two groups were analyzed by unpaired, two-tailed *t*-test. Comparisons among multiple groups were calculated by one-way ANOVA and Bonferroni multiple comparison post-hoc test. Two-way ANOVA was used to analyze the effects of multiple factors. A $p < 0.05$ was considered significant.

3. Results

3.1. Effect of pinocembrin on body weight and mortality after ICH

The mortality of pinocembrin (5 mg/kg)-treated mice was not different from that of vehicle-treated mice (Supplementary Table 1). Mice subjected to the ICH model lost weight in the first 3 days after ICH. Weight gain in pinocembrin-treated mice was significantly greater than that of vehicle-treated mice (Supplementary Fig. 5).

3.2. Pinocembrin ameliorates lesion volume, brain edema and neurologic deficits after ICH

Intravenous administration of pinocembrin (5 and 10 mg/kg) significantly reduced lesion volume on day 3 post-ICH compared with that in vehicle-treated mice (7.11 ± 1.46 mm^3 [5 mg/kg dose] *vs.* 13.56 ± 2.24 mm^3 [vehicle], $p < 0.01$, n = 6; Fig. 1A). Because reduction in lesion volume at 10 mg/kg did not differ from that at 5 mg/kg ($p > 0.05$; Fig. 1A), we used 5 mg/kg of pinocembrin in subsequent studies. We also measured brain tissue water content in striatum and used cerebellum as an internal control. Our results showed that pinocembrin also reduced brain water content in striatum on day 3 post-ICH compared with that in vehicle-treated mice (78.8 ± 1.0% *vs.* 81.4 ± 0.5%, $p < 0.05$, n = 6; Fig. 1B). However, pinocembrin did not alter hematoma size at day 3 or day 5 post-ICH (7.4 ± 1.2 mm^3 *vs.* 7.0 ± 1.7 mm^3 at day 3, and 2.1 ± 0.9 mm^3 *vs.* 2.1 ± 0.8 mm^3 at day 5; both $p > 0.05$; Fig. 1C), indicating that pinocembrin does not affect hematoma clearance after ICH. We next examined the effects of pinocembrin on ICH-induced neurologic deficits. Pinocembrin (5 and 10 mg/kg) significantly reduced neurologic deficit score ($p < 0.001$, n = 10; Fig. 1D), increased falling latency in the wire hanging test ($p < 0.05$, n = 10; Fig. 1E), and decreased the percentage of left turns in the corner turn test ($p < 0.05$, n = 10; Fig. 1F) compared with vehicle treatment on day 3. Moreover, we measured hemoglobin concentration in the striatum at 24 h after ICH, when hematoma reaches a maximum in this model (Chang et al., 2014). No significant difference was found between vehicle-treated and pinocembrin-treated mice (Supplementary Table 2), indicating an equal initial bleeding volume.

3.3. Pinocembrin inhibits microglial activation and proinflammatory cytokine production after ICH

To understand the cellular mechanisms of cerebral protection by pinocembrin, we measured microglial activation and proinflammatory cytokine production after ICH. $CX3CR1^{GFP/+}$ mice were used to visualize microglia. At 24 and 72 h post-ICH, mice were sacrificed, and lysosome marker CD68 was stained to identify reactive microglia. After 24 h, we observed that CD68-positive ($^+$) microglia appeared in the perihematomal region; 72 h later, the number of $CD68^+$ microglia increased markedly ($p < 0.001$, n = 6; Fig. 2A). Almost all $CD68^+$ cells were $CX3CR1/GFP^+$ (Fig. 2A). Pinocembrin significantly reduced the number of $CD68^+$ microglia at both 24 and 72 h compared with the number in the vehicle group (Fig. 2A), indicating that pinocembrin inhibits microglial activation. Moreover, we collected brain tissue from the striatum to determine the M1-associated proinflammatory cytokines. IL-1β (Fig. 2B), IL-6 (Fig. 2C), and TNF-α (Fig. 2D) levels increased markedly after 6 h of injury, but pinocembrin significantly reduced the levels of these cytokines at 6, 24, and 72 h ($p < 0.05$, n = 6).

To confirm whether the effects of pinocembrin on microglia are critical for neuroprotection after ICH, we used clodronate liposome to deplete microglia from the striatum of mice one day before ICH induction (Supplementary Fig. 6A). Notably, pinocembrin did not reduce lesion volume ($p > 0.05$; Supplementary Fig. 6B) or brain water content ($p > 0.05$; Supplementary Fig. 6C) in microglia-depleted mice after ICH.

3.4. Pinocembrin inhibits microglial M1 polarization after ICH

Next, using CX3CR1$^{GFP/+}$ mice, we explored microglial polarization after ICH. Brain sections were immunostained for CD16/32 (M1-like marker) or YM-1 (M2-like marker). Activated microglia were defined based on cell morphology and a cell body diameter cutoff of 7.5 μm (Wang et al., 2008). We observed CD16/32$^+$ microglia dispersed in the perihematomal region at 24 h and 72 h post-ICH. At 72 h post-ICH, the number of CD16/32$^+$ microglia increased compared with that at the 24 h time point, and they were concentrated around the hematoma (n = 6, $p < 0.05$; Fig. 3A). In contrast, YM-1$^+$ microglia were present around the hematoma at 24 h and had significantly increased in number at 72 h (Fig. 3B). Although the number of CD16/32$^+$ microglia was elevated, the proportion of CD16/32$^+$ microglia was lower at 72 h than that at 24 h, whereas the proportion of YM-1$^+$ microglia increased at 72 h. Pinocembrin reduced the proportion of CD16/32$^+$ microglia, but did not change the proportion of YM-1$^+$ microglia.

We next used MACS to sort CD11b$^+$ cells, and collected CD11b$^+$ cell lysate for Western blotting. Our results showed that both iNOS (M1-like marker) and YM-1 were increased at 72 h after ICH, but pinocembrin (5 mg/kg) only decreased iNOS expression (Fig. 3C).

3.5. Pinocembrin protects ICH brain primarily by inhibiting TLR4 activation

TLR4 has been shown to regulate neuroinflammation and affect microglial morphology in the central nervous system. Therefore, to probe the molecular mechanism by which pinocembrin inhibits microglial activation and polarizes M1 microglia, we measured TLR4 expression in the ICH brain. Immunostaining showed that pinocembrin significantly reduced TLR4 expression at 24 h (Fig. 4A). Western blot analysis showed that expression levels of TLR4 and its downstream targets MyD88 and TRIF were elevated at 6 h post-ICH; pinocembrin reduced TLR4 and TRIF expression but did not alter MyD88 expression. At 24 h post-ICH, elevations in TLR4 and MyD88 were reversed by pinocembrin, and at 72 h post-ICH, elevations in TLR4 and TRIF were reversed by pinocembrin (Fig. 4B).

Next, to confirm whether TLR4 is a major molecular target of pinocembrin, we administered pinocembrin (5 mg/kg) to TLR4^{lps}-del mice. On day 3 post-ICH, the injury volume and brain water content were lower in TLR4$^{lps\text{-}del}$ mice than in WT mice (Supplementary Fig. 7A and B). Of note, when compared with two-tailed *t*-test, pinocembrin-treated TLR4$^{lps\text{-}del}$ mice had significantly smaller injury volume (8.75 ± 1.02 mm^3 *vs.* 10.89 ± 1.15 mm^3, $p < 0.05$, n = 6 mice/group; Fig. 4C) and lower brain water content (77.9 ± 0.4% *vs.* 78.9 ± 0.6%, $p < 0.05$, n = 6 mice/group; Fig. 4D) than did the vehicle-treated TLR4$^{lps\text{-}del}$ mice. However, when differences were compared among the four groups with the two-way ANOVA post hoc test (Fig. 4E), the reductions in lesion volume (Fig. 4E) and brain water content (Supplementary Fig. 7C) were not significantly different between pinocembrin- and vehicle-treated TLR4$^{lps\text{-}del}$ mice (both $p > 0.05$). In behavior tests, pinocembrin decreased the neurologic deficit score at 72 h post-ICH ($p < 0.05$, n = 10 mice/-group; Fig. 4F). However, it failed to show an effect in the falling latency test (n = 10; Fig. 4G; falling latency in the TLR4$^{lps\text{-}del}$ sham group: 70 ± 18.5 s at 24 h and 58 ± 12.9 s at 72 h) or corner turn test (Fig. 4H; percentage of left turns in the TLR4$^{lps\text{-}del}$ sham group: 48 ± 3.2% at 24 h and 43 ± 5.1% at 72 h). Together, these results indicate that, even if the protection of

pinocembrin after ICH does not solely depend on inhibition of TLR4 signaling, it is the major mechanism of action of pinocembrin against ICH injury.

3.6. Pinocembrin modulates microglial activation and polarization in TLR4$^{lps\text{-}del}$ mice after ICH

We further investigated the effects of pinocembrin on microglial activation and polarization after ICH in TLR4$^{lps\text{-}del}$ mice. Pinocembrin was administrated to TLR4$^{lps\text{-}del}$ mice at 2 h after ICH. We used Iba1 to stain microglia. Immunostaining for CD68^{+}, CD16/32^{+}, and Ym-1^{+}/Iba1 in the sham TLR4$^{lps\text{-}del}$ mice was similar to that in WT mice. Pinocembrin suppressed microglial activation as evidenced by a reduction in CD68/Iba1 immunoreactivity on day 3 post-ICH ($p < 0.01$, n = 6 mice/group; Fig. 5A). More importantly, it failed to decrease the number of CD16/32^{+} microglia in the ICH brain of the TLR4$^{lps\text{-}del}$ mice ($p > 0.05$, n = 6 mice/group; Fig. 5B), but it increased the number of the YM-1^{+} microglia ($p < 0.05$, n = 6 mice/group; Fig. 5C).

3.7. Pinocembrin mitigates LPS-induced microglial M1 polarization but does not affect microglial phagocytosis of red blood cells in vitro

Microglia can be stimulated by LPS to an M1 phenotype. We cultured both mouse primary microglia and BV-2 microglial cell line to determine whether pinocembrin reduces microglial M1 polarization in vitro. In primary microglia and BV-2 cells stimulated with LPS (50 ng/ml), pretreatment with pinocembrin dose-dependently inhibited secretion of proinflammatory cytokines (IL-1β, IL-6, and TNF-α; n = 5, $p < 0.001$; Fig. 6A and B) and NO production (Fig. 6C and D). Additionally, 10 μM pinocembrin significantly decreased the expression of iNOS in BV-2 cells ($p < 0.01$, n = 5; Fig. 6E). Next, we examined the effects of pinocembrin on microglial phagocytosis of red blood cells in vitro. Our results showed that pinocembrin (10 μM) did not affect the uptake of red blood cells by cultured primary microglia (Supplementary Methods 2 and Supplementary Fig. 8).

To further explore the mechanisms of action of pinocembrin in microglial proinflammatory signaling, we examined the effects of pinocembrin on the NF-κB signaling pathway, which lies downstream of TLR4 and upstream of proinflammatory cytokines and iNOS. Pinocembrin (10 μM) reduced the phosphorylation of NF-κB subunit p65 in the nucleus (pP65, Fig. 6F), decreased levels of phosphorylated IKKα/β (pIKK, Fig. 6G), which complexes with NF-κB, and increased the expression of NF-κB inhibitor IκBα (Fig. 6H). In primary microglia, p65 transcript was seen in the nucleus 30 min after LPS exposure, but pinocembrin (10 μM) almost abolished p65 transcription (Fig. 6I), suggesting that NF-κB is a primary target of pinocembrin under this in vitro condition.

3.8. Pinocembrin decreases TLR4 expression, but not TLR4/MyD88 or TLR4/TRIF interaction in LPS-stimulated microglia

TLR4 regulates IKK expression through MyD88-dependent and -independent pathways. Therefore, we next asked whether TLR4 is a target of pinocembrin in vitro, and how pinocembrin affects TLR4 and its downstream target NF-κB. Our results showed that 1, 3, and 10 μM pinocembrin significantly reduced TLR4 expression in LPS-stimulated BV-2 cells (Fig. 7A). Immunostaining for TLR4 in pinocembrin-treated primary microglia showed

a similar trend toward a decrease in LPS-induced TLR4 compared to that with LPS alone (Fig. 7D).

To further study the effect of pinocembrin on the relationship between TLR4 and NF-κB, we silenced TLR4 with siRNA in the BV-2 cell line (Supplementary Fig. 4). In control cells that were transfected with scrambled siRNA, 30 min of LPS stimulation caused a sharp increase in pP65 expression that was reduced markedly by 10 μM pinocembrin. TLR4 siRNA transfection significantly reduced LPS-stimulated NF-κB activation. When BV-2 cells were co-treated with TLR4 siRNA and pinocembrin, the phosphorylation of p65 was further reduced (Fig. 7B), indicating that TLR4 might be a primary target of pinocembrin, but not the sole regulator of the NF-κB signaling pathway.

Finally, we investigated the effect of pinocembrin on crosstalk between TLR4 and NF-κB by performing immunoprecipitation to determine whether pinocembrin influences the interaction between TLR4 and MyD88 or TRIF. The interaction between TLR4 and MyD88/TRIF did not differ significantly between the LPS group and the pinocembrin group (Fig. 7C, Supplementary Fig. 9), suggesting that pinocembrin only decreases TLR4 expression without affecting its interaction with MyD88 or TRIF.

4. Discussion

This is the first study to test the efficacy of pinocembrin in a mouse model of ICH and to elucidate its potential mechanism of action. We showed that pinocembrin improved early ICH outcomes at 72 h in vivo. However, it did not affect hematoma clearance in WT mice and failed to ameliorate early ICH injury in microglia-depleted mice. Pinocembrin inhibited TLR4 expression in WT mice but only minimally reduced injury volume, brain edema, and neurologic deficits in $TLR4^{lps\text{-}del}$ mice with ICH. Furthermore, pinocembrin decreased microglial activation and proinflammatory cytokine production at 6, 24, and 72 h post-ICH in WT mice. Notably, pinocembrin suppressed microglial polarization to M1 phenotype. In $TLR4^{lps\text{-}del}$ mice, although pinocembrin failed to decrease M1 microglia, it reduced microglial activation and increased M2 phenotype microglia. In vitro, pinocembrin inhibited proinflammatory cytokine production in LPS-stimulated BV-2 cells and primary microglia, but it did not affect microglial phagocytosis of red blood cells. Additionally, it reduced TLR4 expression in vitro, which led to the downregulation of NF-κB activation. This action decreased phosphorylated IKK, increased IκB expression, and interfered with NF-κB transcription but did not interfere with the interaction between TLR4 and MyD88 or TRIF. These novel findings indicate that TLR4 is a major target of pinocembrin and that decreases in M1 phenotype microglia are critical for protection by pinocembrin against ICH injury (Fig. 8).

Pinocembrin acts at multiple targets (Lan et al., 2016) and has been shown to offer protection after cerebral ischemia (Shi et al., 2011; Wu et al., 2013). We demonstrated here that pinocembrin can significantly improve neurologic function, lessen brain injury volume, and decrease brain water content of ICH mice in vivo. These results provide a strong rationale for pinocembrin to be used in ICH treatment. In vivo, pinocembrin decreased the expression of TLR4, MyD88, and TRIF, and in vitro, it also reduced TLR4 expression and

downregulated the NF-κB signaling pathway. Although pinocembrin-treated TLR4$^{lps\text{-}del}$ mice exhibited a statistically significant reduction in injury volume and brain edema after ICH when compared to vehicle-treated TLR4$^{lps\text{-}del}$ mice (analyzed by two-tailed *t*-test), the differences disappeared when we performed a two-way ANOVA post-hoc test among the four groups (WT+Veh, WT+Pino, TLR4$^{lps\text{-}del}$+Veh, and TLR4$^{lps\text{-}del}$+Pino). These data indicate that pinocembrin primarily targets TLR4, although its protection against ICH might be not solely dependent on TLR4 activation. It is unknown whether TLR4 activation modulates microglial M1 polarization after ICH.

Although pinocembrin was reported to have an anti-inflammatory effect in the central nervous system (Cheng et al., 2016; Gao et al., 2010), it is unclear whether it targets microglia. Cellular inflammatory responses, and microglial activation in particular, contribute to ICH-induced secondary brain injury (Wang and Dore, 2007; Wu et al., 2010). We have shown previously that inhibition of microglial activation improves histologic and functional outcomes after ICH (Wang et al., 2003; Wang and Tsirka, 2005). However, when striatal microglia were depleted by clodronate liposome, pinocembrin did not reduce injury volume or brain water content after ICH. This finding supports the notion that changes in microglial polarity underlie the protective action of pinocembrin. We provide evidence in this study that pinocembrin effectively decreases the number of CD68^{+} microglia in the peri-ICH region, indicating that it can inhibit microglial activation after ICH. Moreover, pinocembrin inhibits proinflammatory cytokine levels (IL-1β, IL-6, and TNF-α) in vivo and in LPS-stimulated M1 microglia in vitro. Therefore, additional study of the effects of pinocembrin on microglial polarization will be particularly important.

In a blood injection model of ICH (Wan et al., 2016), global expression of CD16 and iNOS was increased after 4 h, and CD206 and YM-1 expression was increased after 24 h. On day 4 post-ICH, mRNA levels of proinflammatory cytokines were upregulated, whereas M2 markers did not exhibit a significant change. However, the time course of change in specific microglial M1-/M2-like polarization is still unknown. In our study, we found that both M1-like (CD16/32) and M2-like (YM-1) markers began to be expressed in CX3CR1^{+} microglia at 24 h after injury. In addition, the changes in M1-like and M2-like markers showed different trends. Specifi-cally, on day 1, most of the microglia migrating to or activated around the hematoma were M1 phenotype. After 3 days, although the total number of M1 microglia was higher than it had been on day 1, the percentage of M1 microglia was decreased, and the percentage of M2 microglia was increased. The fact that the number of activated microglia (CD68^{+}) increased from day 1 to day 3 indicates that microglia might experience an M1-to-M2 transition in the first 3 days post-ICH.

After transient cerebral ischemia, M1 microglia increase from day 3 onward, whereas M2 microglia start to appear on day 1 and persist for 7 days (Hu et al., 2012). In recent years, it was reported that an M2-to-M1 microglia/macrophage switch occurs in spinal cord injury (Kigerl et al., 2009) and ischemic stroke (Hu et al., 2012), whereas a mixed M1 and M2 population is seen in traumatic brain injury (Morganti et al., 2016; Zanier et al., 2016). The microglial M1-to-M2 phenotype transition we observed in the ICH brain may result from phenotypic transformation of microglia in the early stage of ICH or result from M2-like

microglial migration or M2-like macrophage infiltration. These possibilities deserve further study.

In the ICH brain, TLR4 is upregulated mainly in microglia (Lively and Schlichter, 2012). The deletion of TLR4 improves ICH outcomes via inhibition of the NF-κB signaling pathway in the blood-injection ICH model (Lively and Schlichter, 2012). Furthermore, TLR4 activation has been shown to be essential for M1 microglial polarization in glioma stem cells in vivo (a Dzaye et al., 2016) and in BV-2 cells in vitro (Gong et al., 2016; Wang et al., 2016). Our data show that pinocembrin decreases M1 phenotype micro-glia, as evidenced by decreases in the number of the $CD16/32^{+}$ microglia and iNOS expression in MACS-sorted $CD11b^{+}$ microglia. However, this effect of pinocembrin was abolished in $TLR4^{lps\text{-}del}$ mice with ICH, indicating that pinocembrin reduced microglial M1 polarization mainly by TLR4 inhibition.

M2 phenotype microglia have been demonstrated to be efficient phagocytes in brain. Anti-inflammatory cytokine IL-4 is able to promote the cleanup of ischemic debris by stimulating microglial M2 polarization (Zhao et al., 2015a). In an Alzheimer's disease model, Aβ plagues are phagocytosed and cleared by M2 phenotype microglia (Mandrekar-Colucci et al., 2012). In our study, pinocembrin did not affect hematoma clearance in vivo or phagocytosis of red blood cells in vitro. These results are supported by our data showing that pinocembrin does not change the proportion of M2 phenotype microglia in WT mice. Interestingly, pinocembrin was able to increase M2 ($YM\text{-}1^{+}$) phenotype microglia when TLR4 was deleted. This result suggests that pinocembrin might have the potential to promote microglial M2 polarization but that this capability is inhibited by the activation of TLR4 in the ICH brain of WT mice.

We demonstrated in vitro that pinocembrin inhibits NF-κB translocation by decreasing phosphorylated IKKα/β, thus causing an increase in IκB expression. This activity can be explained by the pinocembrin-induced reduction of TLR4 expression. We further used immunoprecipitation to measure the interaction between TLR4 and MyD88 or TRIF. Interestingly, pinocembrin did not affect MyD88 or TRIF interaction with TLR4, indicating that pinocembrin does not act through a MyD88- or TRIF-dependent mechanism, but only by inhibiting TLR4 expression. Moreover, when TLR4 was silenced, pinocembrin was still able to downregulate the phosphorylation of p65 in LPS-stimulated BV-2 cells. This finding suggests that pinocembrin might not solely target TLR4 in vitro. Together with our in vivo results obtained in TLR4-deleted mice, our data provide rationale to explore whether pinocembrin has other targets that promote microglial polarization to M2 phenotype.

In summary, we provide the first preclinical evidence that pinocembrin protects ICH brain primarily by inhibiting TLR4 activation and microglial M1 polarization. These findings imply that pinocembrin may hold potential for treating ICH and other acute brain injuries. Additionally, we characterized microglial activation and polarization at early time points after ICH. Modulation of microglial polarization after ICH might warrant additional study as a potential new therapeutic approach.

Supplementary Material

Refer to Web version on PubMed Central for supplementary material.

Acknowledgments

The authors thank Weizhu Tang for technical assistance; Wenzhu Wang for blind analysis of behavior experiments and immunostaining; and Claire Levine for assistance with manuscript preparation. We thank Dr. Guanhua Du for kindly supplying pinocembrin compound. We thank Raymond Koehler, Zengjin Yang, and all Wang lab members for constructive suggestions. This work was supported by AHA Mid-Atlantic Affiliate Grant-in-Aid 13GRNT15730001, NIH R01NS078026, and R01AT007317 (JW), an AHA Mid-Atlantic Affiliate Postdoctoral Fellowship Award 15POST25090114 (XL), and a “Stimulating and Advancing ACCM Research (StAAR)” grant from the Department of Anesthesiology and Critical Care Medicine, Johns Hopkins Medicine (JW).

Appendix A. Supplementary data

Supplementary data associated with this article can be found, in the online version, at http://dx.doi.org/10.1016/j.bbi.2016.12.012.

Abbreviations

DAPI	4/6-diamidino-2-phenylindole
FBS	fetal bovine serum
HP-β-CD	hydroxypropyl-β-cyclodextrin
ICH	intracerebral hemorrhage
IKK	IκB kinase
IL-1β	interleukin-1β
IL-6	interleukin-6
IκB	Inhibitor of κB
LPS	lipopolysaccharide
MACS	magnetic-activated cell sorting
NO	nitric oxide
siRNA	small interfering RNA
TLR	toll-like receptor
TNF-α	tumor necrosis factor-α

References

a Dzaye OD, Hu F, Derkow K, Haage V, Euskirchen P, Harms C, Lehnardt S, Synowitz M, Wolf SA, Kettenmann H. Glioma Stem Cells but Not Bulk Glioma Cells Upregulate IL-6 Secretion in Microglia/Brain Macrophages via Toll-like Receptor 4 Signaling. J Neuropathol Exp Neurol. 2016; 75:429–440. [PubMed: 27030742]

Avila M, Gonzalez-Espinosa C. Signaling through Toll-like receptor 4 and mast cell-dependent innate immunity responses. IUBMB Life. 2011; 63:873–880. [PubMed: 21905201]

Bal-Price A, Brown GC. Inflammatory neurodegeneration mediated by nitric oxide from activated glia-inhibiting neuronal respiration, causing glutamate release and excitotoxicity. J Neurosci. 2001; 21:6480–6491. [PubMed: 11517237]

Blasi E, Barluzzi R, Bocchini V, Mazzolla R, Bistoni F. Immortalization of murine microglial cells by a v-raf/v-myc carrying retrovirus. J Neuroimmunol. 1990; 27:229–237. [PubMed: 2110186]

Bocchini V, Mazzolla R, Barluzzi R, Blasi E, Sick P, Kettenmann H. An immortalized cell line expresses properties of activated microglial cells. J Neurosci Res. 1992; 31:616–621. [PubMed: 1578513]

Boche D, Perry VH, Nicoll JA. Review: activation patterns of microglia and their identification in the human brain. Neuropathol Appl Neurobiol. 2013; 39:3–18. [PubMed: 23252647]

Chang CF, Cho S, Wang J. (−)-Epicatechin protects hemorrhagic brain via synergistic Nrf2 pathways. Ann Clin Transl Neurol. 2014; 1:258–271. [PubMed: 24741667]

Cheng T, Wang W, Li Q, Han X, Xing J, Qi C, Lan X, Wan J, Potts A, Guan F, Wang J. Cerebroprotection of flavanol (−)-epicatechin after traumatic brain injury via Nrf2-dependent and -independent pathways. Free Radic Biol Med. 2016; 92:15–28. [PubMed: 26724590]

Drew PD, Chavis JA. The cyclopentone prostaglandin 15-deoxy-Delta (12,14) prostaglandin J2 represses nitric oxide, TNF-alpha, and IL-12 production by microglial cells. J Neuroimmunol. 2001; 115:28–35. [PubMed: 11282151]

Fang H, Chen J, Lin S, Wang P, Wang Y, Xiong X, Yang Q. CD36-mediated hematoma absorption following intracerebral hemorrhage: negative regulation by TLR4 signaling. J Immunol. 2014; 192:5984–5992. [PubMed: 24808360]

Fernandez-Lopez D, Faustino J, Klibanov AL, Derugin N, Blanchard E, Simon F, Leib SL, Vexler ZS. Microglial Cells Prevent Hemorrhage in Neonatal Focal Arterial Stroke. J Neurosci. 2016; 36:2881–2893. [PubMed: 26961944]

Gao M, Zhu SY, Tan CB, Xu B, Zhang WC, Du GH. Pinocembrin protects the neurovascular unit by reducing inflammation and extracellular proteolysis in MCAO rats. J Asian Nat Prod Res. 2010; 12:407–418. [PubMed: 20496198]

Garcia-Bonilla L, Benakis C, Moore J, Iadecola C, Anrather J. Immune mechanisms in cerebral ischemic tolerance. Front Neurosci. 2014; 8:44. [PubMed: 24624056]

Gong L, Wang H, Sun X, Liu C, Duan C, Cai R, Gu X, Zhu S. Toll-Interleukin 1 Receptor domain-containing adaptor protein positively regulates BV2 cell M1 polarization. Eur J Neurosci. 2016; 43:1674–1682. [PubMed: 27061018]

Han X, Lan X, Li Q, Gao Y, Zhu W, Cheng T, Maruyama T, Wang J. Inhibition of prostaglandin E2 receptor EP3 mitigates thrombin-induced brain injury. J Cereb Blood Flow Metab. 2016; 36:1059–1074. [PubMed: 26661165]

Held-Feindt J, Hattermann K, Muerkoster SS, Wedderkopp H, Knerlich-Lukoschus F, Ungefroren H, Mehdorn HM, Mentlein R. CX3CR1 promotes recruitment of human glioma-infiltrating microglia/macrophages (GIMs). Exp Cell Res. 2010; 316:1553–1566. [PubMed: 20184883]

Hu X, Li P, Guo Y, Wang H, Leak RK, Chen S, Gao Y, Chen J. Microglia/macrophage polarization dynamics reveal novel mechanism of injury expansion after focal cerebral ischemia. Stroke. 2012; 43:3063–3070. [PubMed: 22933588]

Kigerl KA, Gensel JC, Ankeny DP, Alexander JK, Donnelly DJ, Popovich PG. Identification of two distinct macrophage subsets with divergent effects causing either neurotoxicity or regeneration in the injured mouse spinal cord. J Neurosci. 2009; 29:13435–13444. [PubMed: 19864556]

Kong Y, Le Y. Toll-like receptors in inflammation of the central nervous system. Int Immunopharmacol. 2011; 11:1407–1414. [PubMed: 21600311]

Lan X, Liu R, Sun L, Zhang T, Du G. Methyl salicylate 2-O-beta-D-lactoside, a novel salicylic acid analogue, acts as an anti-inflammatory agent on microglia and astrocytes. J Neuroinflammation. 2011; 8:98. [PubMed: 21831328]

Lan X, Wang W, Li Q, Wang J. The natural flavonoid pinocembrin: molecular targets and potential therapeutic applications. Mol Neurobiol. 2016; 53:1794–1801. [PubMed: 25744566]

Lee MY, Lufkin T. Development of the “Three-step MACS”: a novel strategy for isolating rare cell populations in the absence of known cell surface markers from complex animal tissue. J Biomol Technol. 2012; 23:69–77.

Liu R, Gao M, Yang ZH, Du GH. Pinocembrin protects rat brain against oxidation and apoptosis induced by ischemia-reperfusion both in vivo and in vitro. Brain Res. 2008; 1216:104–115. [PubMed: 18495093]

Liu R, Wu CX, Zhou D, Yang F, Tian S, Zhang L, Zhang TT, Du GH. Pinocembrin protects against beta-amyloid-induced toxicity in neurons through inhibiting receptor for advanced glycation end products (RAGE)-independent signaling pathways and regulating mitochondrion-mediated apoptosis. BMC Med. 2012; 10:105. [PubMed: 22989295]

Liu R, Li JZ, Song JK, Zhou D, Huang C, Bai XY, Xie T, Zhang X, Li YJ, Wu CX, Zhang L, Li L, Zhang TT, Du GH. Pinocembrin improves cognition and protects the neurovascular unit in Alzheimer related deficits. Neurobiol Aging. 2014; 35:1275–1285. [PubMed: 24468471]

Lively S, Schlichter LC. Age-related comparisons of evolution of the inflammatory response after intracerebral hemorrhage in rats. Transl Stroke Res. 2012; 3:132–146. [PubMed: 22707991]

Mandrekar-Colucci S, Karlo JC, Landreth GE. Mechanisms underlying the rapid peroxisome proliferator-activated receptor-gamma-mediated amyloid clearance and reversal of cognitive deficits in a murine model of Alzheimer’s disease. J Neurosci. 2012; 32:10117–10128. [PubMed: 22836247]

Meng F, Liu R, Gao M, Wang Y, Yu X, Xuan Z, Sun J, Yang F, Wu C, Du G. Pinocembrin attenuates blood-brain barrier injury induced by global cerebral ischemia-reperfusion in rats. Brain Res. 2011; 1391:93–101. [PubMed: 21435338]

Miron VE, Boyd A, Zhao JW, Yuen TJ, Ruckh JM, Shadrach JL, van Wijngaarden P, Wagers AJ, Williams A, Franklin RJ, ffrench-Constant C. M2 microglia and macrophages drive oligodendrocyte differentiation during CNS remyelination. Nat Neurosci. 2013; 16:1211–1218. [PubMed: 23872599]

Morganti JM, Riparip LK, Rosi S. Call Off the Dog(ma): M1/M2 Polarization Is Concurrent following Traumatic Brain Injury. PLoS ONE. 2016; 11:e0148001. [PubMed: 26808663]

Morgenstern LB, Hemphill JC 3rd, Anderson C, Becker K, Broderick JP, Connolly ES Jr, Greenberg SM, Huang JN, MacDonald RL, Messe SR, Mitchell PH, Selim M, Tamargo RJ, American Heart Association Stroke, C., Council on Cardiovascular, N. Guidelines for the management of spontaneous intracerebral hemorrhage: a guideline for healthcare professionals from the American Heart Association/American Stroke Association. Stroke. 2010; 41:2108–2129. [PubMed: 20651276]

Palacio S, Hart RG. Regarding article “Guidelines for the management of spontaneous intracerebral hemorrhage: a guideline for healthcare professionals from the American Heart Association/American Stroke Association”. Stroke. 2011; 42:e23. [PubMed: 21193753]

Perego C, Fumagalli S, De Simoni MG. Temporal pattern of expression and colocalization of microglia/macrophage phenotype markers following brain ischemic injury in mice. J Neuroinflammation. 2011; 8:174. [PubMed: 22152337]

Rodriguez-Yanez M, Brea D, Arias S, Blanco M, Pumar JM, Castillo J, Sobrino T. Increased expression of Toll-like receptors 2 and 4 is associated with poor outcome in intracerebral hemorrhage. J Neuroimmunol. 2012; 247:75–80. [PubMed: 22498099]

Shechter R, Schwartz M. Harnessing monocyte-derived macrophages to control central nervous system pathologies: no longer ‘if’ but ‘how’. J Pathol. 2013; 229:332–346. [PubMed: 23007711]

Shi LL, Chen BN, Gao M, Zhang HA, Li YJ, Wang L, Du GH. The characteristics of therapeutic effect of pinocembrin in transient global brain ischemia/reperfusion rats. Life Sci. 2011; 88:521–528. [PubMed: 21262238]

Wan S, Cheng Y, Jin H, Guo D, Hua Y, Keep RF, Xi G. Microglia Activation and Polarization After Intracerebral Hemorrhage in Mice: the Role of Protease-Activated Receptor-1. Transl Stroke Res. 2016; 7:478–487. [PubMed: 27206851]

Wang J, Dore S. Heme oxygenase-1 exacerbates early brain injury after intracerebral haemorrhage. Brain. 2007; 130:1643–1652. [PubMed: 17525142]

Wang J, Tsirka SE. Neuroprotection by inhibition of matrix metalloproteinases in a mouse model of intracerebral haemorrhage. Brain. 2005; 128:1622–1633. [PubMed: 15800021]

Wang J, Rogove AD, Tsirka AE, Tsirka SE. Protective role of tuftsin fragment 1–3 in an animal model of intracerebral hemorrhage. Ann Neurol. 2003; 54:655–664. [PubMed: 14595655]

Wang J, Fields J, Dore S. The development of an improved preclinical mouse model of intracerebral hemorrhage using double infusion of autologous whole blood. Brain Res. 2008; 1222:214–221. [PubMed: 18586227]

Wang SB, Pang XB, Gao M, Fang LH, Du GH. Pinocembrin protects rats against cerebral ischemic damage through soluble epoxide hydrolase and epoxyeicosatrienoic acids. Chin J Nat Med. 2013a; 11:207–213. [PubMed: 23725831]

Wang YC, Wang PF, Fang H, Chen J, Xiong XY, Yang QW. Toll-like receptor 4 antagonist attenuates intracerebral hemorrhage-induced brain injury. Stroke. 2013b; 44:2545–2552. [PubMed: 23839500]

Wang H, Liu C, Han M, Cheng C, Zhang D. TRAM1 Promotes Microglia M1 Polarization. J Mol Neurosci. 2016; 58:287–296. [PubMed: 26563450]

Wu H, Zhang Z, Hu X, Zhao R, Song Y, Ban X, Qi J, Wang J. Dynamic changes of inflammatory markers in brain after hemorrhagic stroke in humans: a postmortem study. Brain Res. 2010; 1342:111–117. [PubMed: 20420814]

Wu H, Wu T, Li M, Wang J. Efficacy of the lipid-soluble iron chelator 2,2′-dipyridyl against hemorrhagic brain injury. Neurobiol Dis. 2012; 45:388–394. [PubMed: 21930208]

Wu CX, Liu R, Gao M, Zhao G, Wu S, Wu CF, Du GH. Pinocembrin protects brain against ischemia/reperfusion injury by attenuating endoplasmic reticulum stress induced apoptosis. Neurosci Lett. 2013; 546:57–62. [PubMed: 23669639]

Yang ZH, Sun X, Qi Y, Mei C, Sun XB, Du GH. Uptake characteristics of pinocembrin and its effect on p-glycoprotein at the blood-brain barrier in in vitro cell experiments. J Asian Nat Prod Res. 2012; 14:14–21. [PubMed: 22263589]

Yuan B, Shen H, Lin L, Su T, Huang Z, Yang Z. Scavenger receptor SRA attenuates TLR4-induced microglia activation in intracerebral hemorrhage. J Neuroimmunol. 2015; 289:87–92. [PubMed: 26616876]

Zanier ER, Marchesi F, Ortolano F, Perego C, Arabian M, Zoerle T, Sammali E, Pischiutta F, De Simoni MG. Fractalkine receptor deficiency is associated with early protection but late worsening of outcome following brain trauma in mice. J Neurotrauma. 2016; 33:1060–1072. [PubMed: 26180940]

Zhang, Z., Zhang, Z., Lu, H., Yang, Q., Wu, H., Wang, J. Microglial polarization and inflammatory mediators after intracerebral hemorrhage. Mol Neurobiol. 2016. http://dx.doi.org/10.1007/s12035-12016-19785-12036. in press

Zhao G, Zhang W, Li L, Wu S, Du G. Pinocembrin protects the brain against ischemia-reperfusion injury and reverses the autophagy dysfunction in the penumbra area. Molecules. 2014; 19:15786–15798. [PubMed: 25271424]

Zhao X, Wang H, Sun G, Zhang J, Edwards NJ, Aronowski J. Neuronal interleukin-4 as a modulator of microglial pathways and ischemic brain damage. J Neurosci. 2015a; 35:11281–11291. [PubMed: 26269636]

Zhao X, Wu T, Chang CF, Wu H, Han X, Li Q, Gao Y, Li Q, Hou Z, Maruyama T, Zhang J, Wang J. Toxic role of prostaglandin E2 receptor EP1 after intracerebral hemorrhage in mice. Brain Behav Immun. 2015b; 46:293–310. [PubMed: 25697396]

Zhu W, Gao Y, Chang CF, Wan JR, Zhu SS, Wang J. Mouse models of intracerebral hemorrhage in ventricle, cortex, and hippocampus by injections of autologous blood or collagenase. PLoS ONE. 2014; 9:e97423. [PubMed: 24831292]

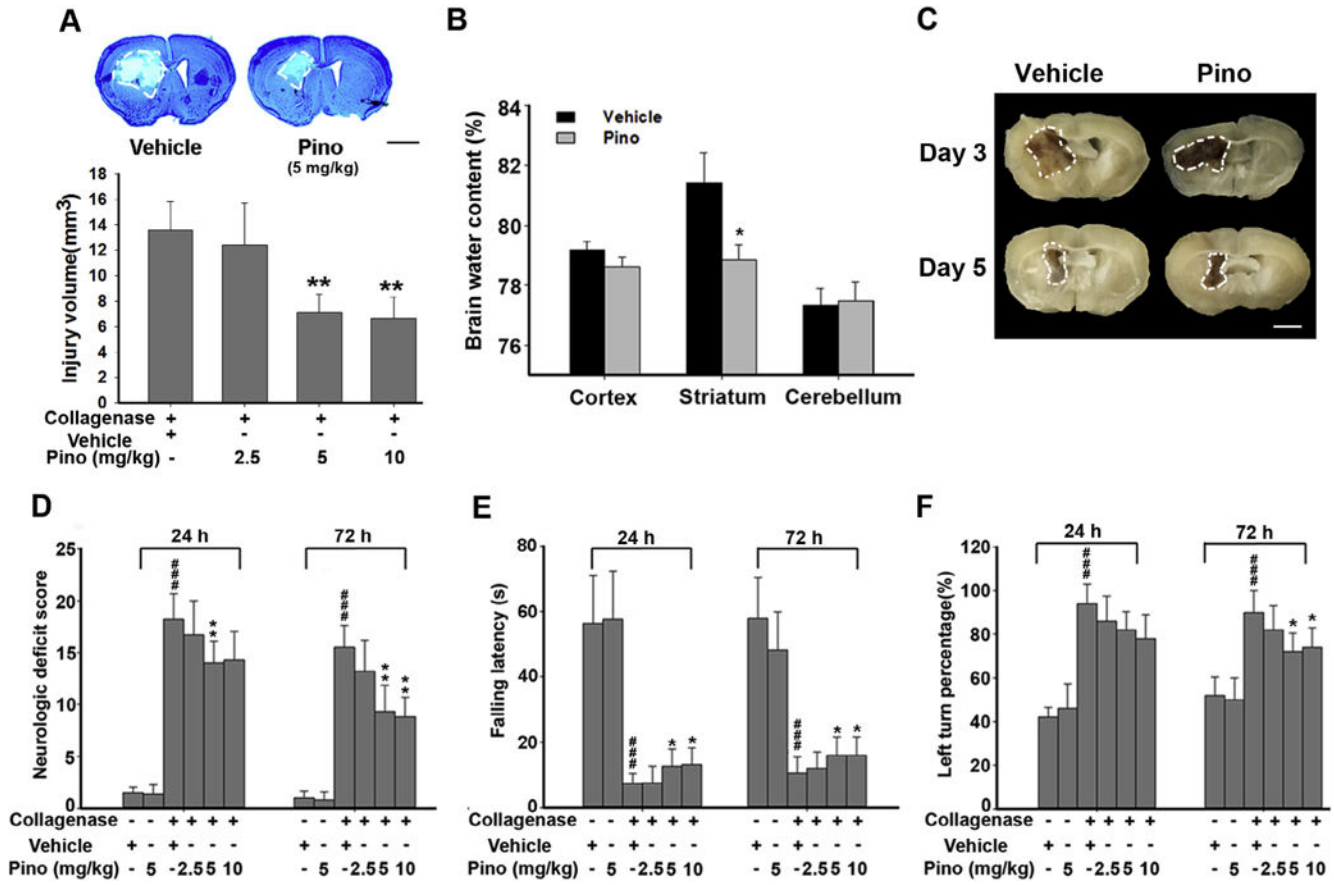

Fig. 1.

Pinocembrin improves functional and histologic outcomes in mice subjected to ICH. (A) Injury volume was determined by staining brain sections with Luxol fast blue. Pinocembrin (5 and 10 mg/kg) decreased the injury volume on day 3 post-ICH; n = 6 mice/group. Scale bar = 2 mm. (B) Pinocembrin (5 mg/kg) reduced brain water content in the ipsilateral striatum compared with that in vehicle-treated controls; n = 6 mice/group. (C) Pinocembrin (5 mg/kg) did not reduce hematoma size on days 3 and 5 post-ICH. Scale bar = 1 mm. (D) Neurologic deficit score evaluation (n = 10 mice/group). (E) Wire hanging test (n = 10 mice/group). (F) Corner turn test (n = 10 mice/group). $^{###}p < 0.001$ *vs.* sham group; $^{*}p < 0.05$, $^{**}p < 0.01$, $^{***}p < 0.001$ *vs.* vehicle group. All data are presented as mean ± S.D.

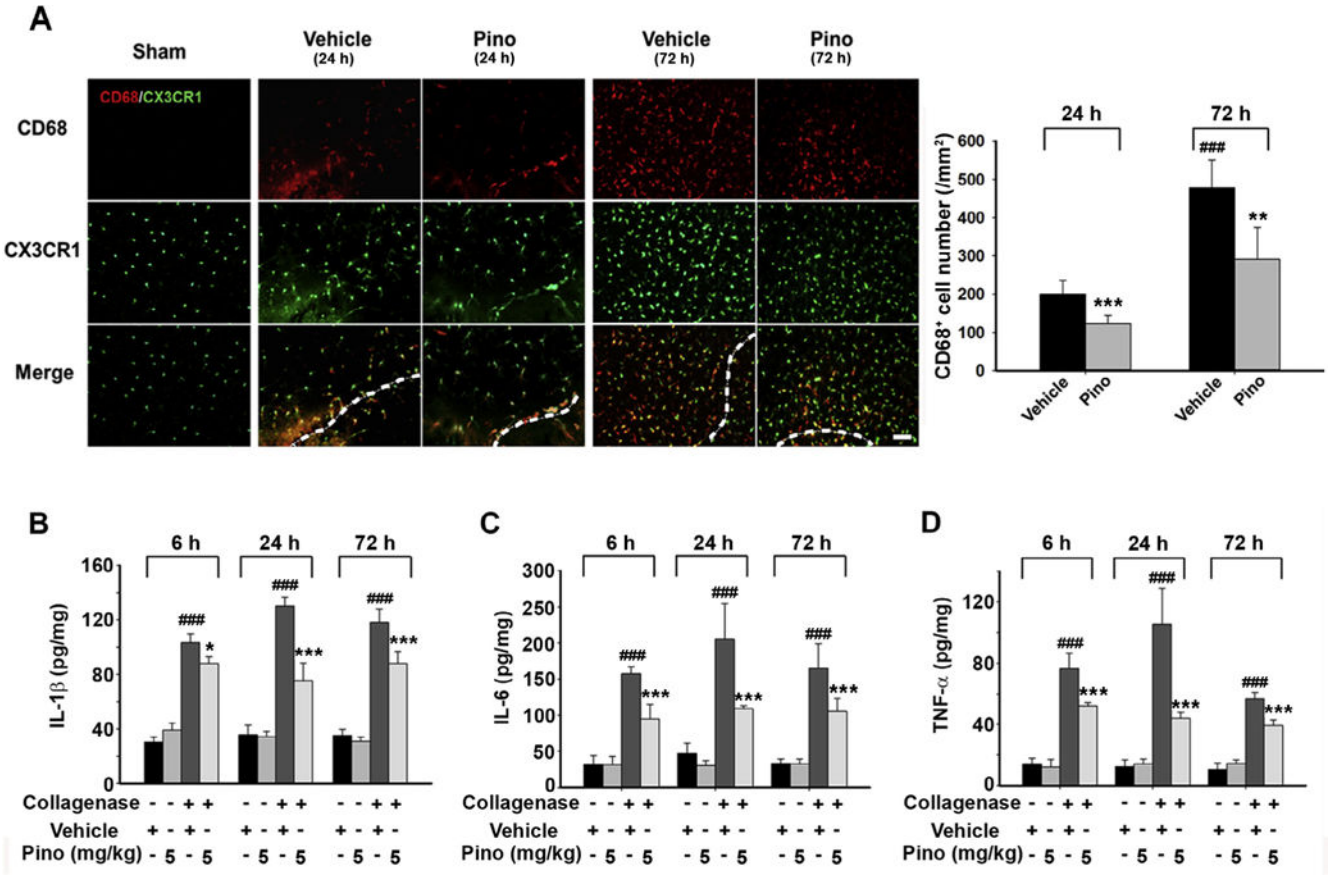

Fig. 2.

Pinocembrin inhibits microglial activation and proinflammatory cytokine production in mice subjected to ICH. All image analysis was performed in the perihematomal region, which was defined within one 20 field that corresponded to 460 μm from the edge of the hematoma (white lines indicate the border of the hematoma). (A) Fewer $CD68^+$ (red) microglia (CX3CR1, green) were present in ICH brain from pinocembrin-treated mice than in ICH brain from vehicle-treated mice. $^{###}p < 0.001$ *vs.* 24 h vehicle group; $*p < 0.05$, $***p < 0.001$ *vs.* the vehicle group at the same time point. Scale bar = 40 μm. Pinocembrin suppressed proinflammatory cytokines IL-1β (B), IL-6 (C), and TNF-α (D) at 6, 24, and 72 h post-ICH. $^{###}p < 0.001$ *vs.* sham group; $*p < 0.05$, $***p < 0.001$ *vs.* the corresponding vehicle group. All data are presented as mean ± S.D.; n = 6 mice/group. (For interpretation of the references to color in this figure legend, the reader is referred to the web version of this article.)

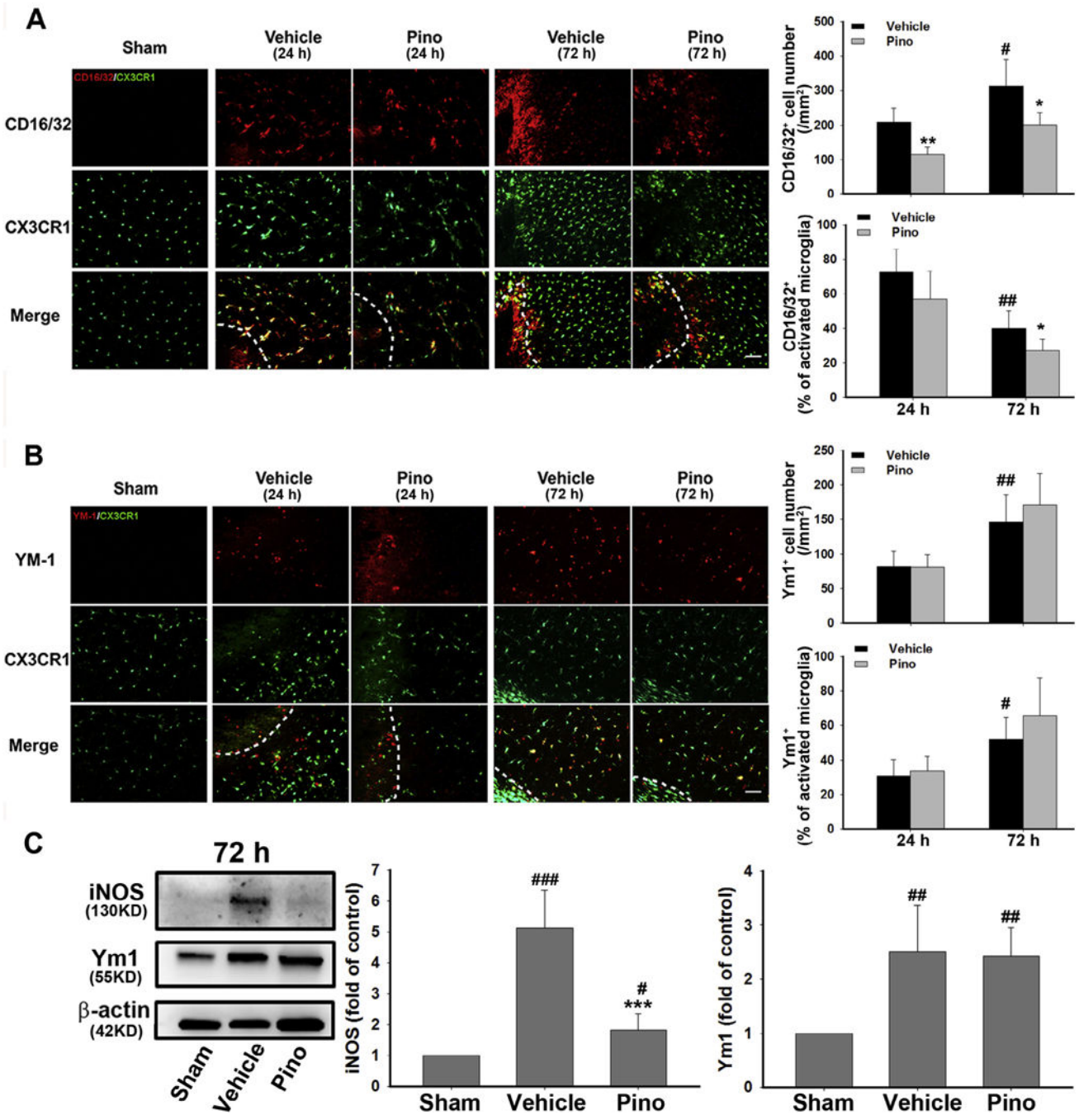

Fig. 3.

Pinocembrin suppresses M1 phenotype microglia in mice subjected to ICH. (A) Immunostaining of CD16/32 (red) in brain sections at 24 and 72 h post-ICH. (B) Immunostaining of YM-1 (red) in brain sections at 24 and 72 h post-ICH. $^{\#}p < 0.05$, $^{\#\#}p < 0.01$ *vs.* vehicle group at 24 h; $^{*}p < 0.05$, $^{**}p < 0.01$ *vs.* corresponding vehicle group. White lines in A and B indicate the border of the hematoma. (C) Magnetic-activated cell sorting of microglia was used to determine the expression of M1 and M2 markers in $CD11b^{+}$ cells. Western blotting was used to analyze iNOS and YM-1 expression. $^{\#}p < 0.05$, $^{\#\#}p <$

0.01, ###$p < 0.001$ *vs.* sham group; ***$p < 0.001$ *vs.* vehicle group. All data are presented as mean ± S.D.; n = 6 mice/group. Scale bar = 40 μm.

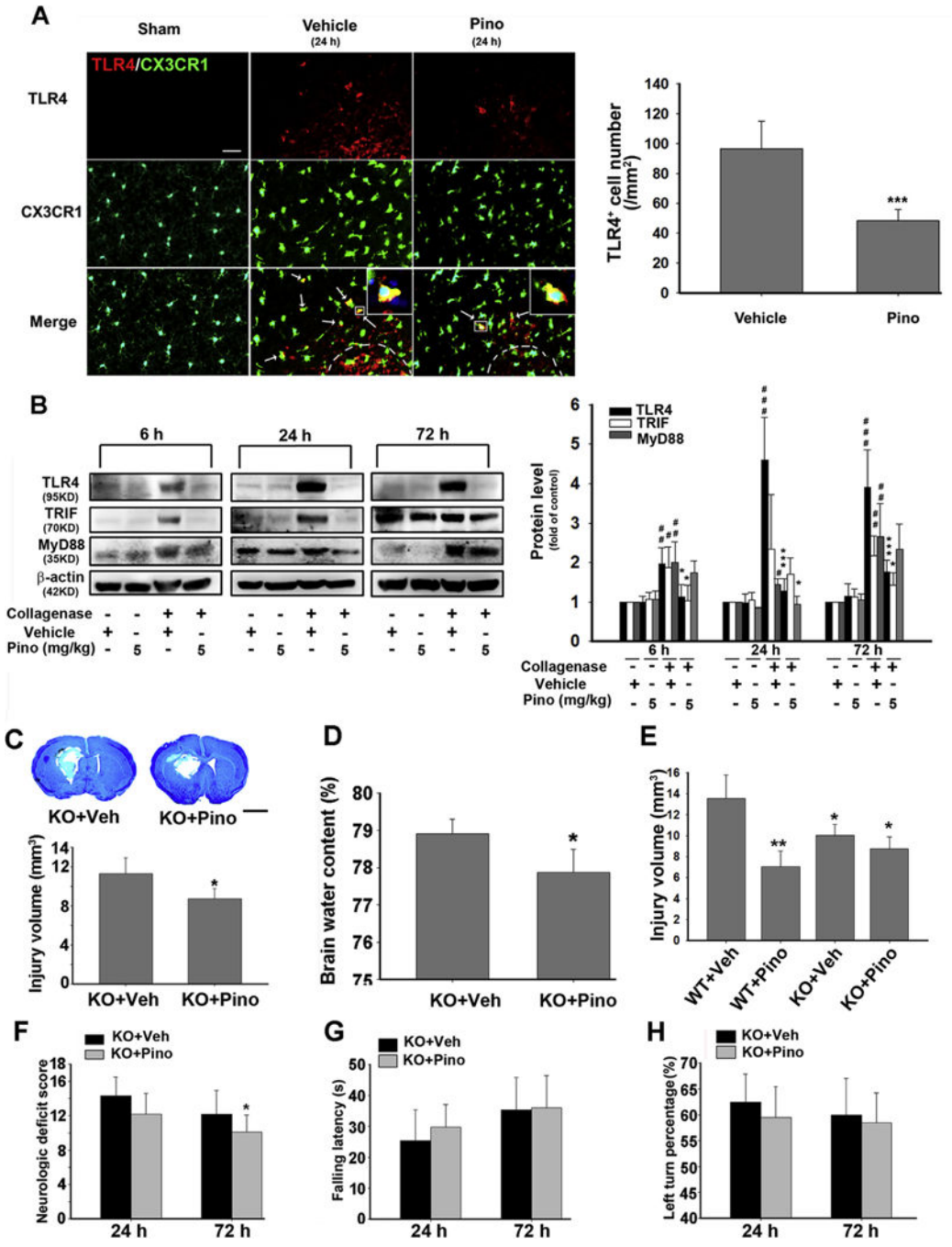

Fig. 4.

Pinocembrin decreases TLR4 expression in WT mice subjected to ICH and has limited protection in TLR4$^{lps\text{-}del}$ mice. (A) Immunostaining of TLR4 (red) in brain sections at 24 h post-ICH. White lines indicate the border of the hematoma. Red: TLR4, green: CX3CR1, blue: DAPI. n = 6 mice/group; ***$p < 0.001$ *vs.* vehicle group. Scale bar = 40 μm. (B) Pinocembrin reduced the expression of TLR4, TRIF, and MyD88 post-ICH compared to that in vehicle-treated mice. n = 6 mice/group; $^{\#}p < 0.05$, $^{\#\#}p < 0.01$, $^{\#\#\#}p < 0.001$ *vs.* sham group; *$p < 0.05$, **$p < 0.01$, ***$p < 0.001$ *vs.* vehicle group. (C) Injury volume in

TLR4$^{lps\text{-}del}$ (KO) mice treated with vehicle or pinocembrin. n = 6 mice/group; *$p < 0.05$ *vs.* vehicle-treated KO mice. Scale bar = 2 mm. (D) Ipsilateral striatum water content. n = 6 mice/group; *$p < 0.05$ *vs.* vehicle-treated KO mice. (E) Injury volume in wild-type (WT) mice and KO mice treated with vehicle or pinocembrin (5 mg/kg). *$p < 0.05$, **$p < 0.01$ *vs.* vehicle-treated WT mice (Veh). (F) Neurologic deficit score evaluation. n = 10 mice/group; *$p < 0.05$ *vs.* vehicle-treated KO mice. (G) Wire hanging test. n = 10 mice/group. (H) Corner turn test. n = 10 mice/group. All data are presented as mean ± S.D. (For interpretation of the references to color in this figure legend, the reader is referred to the web version of this article.)

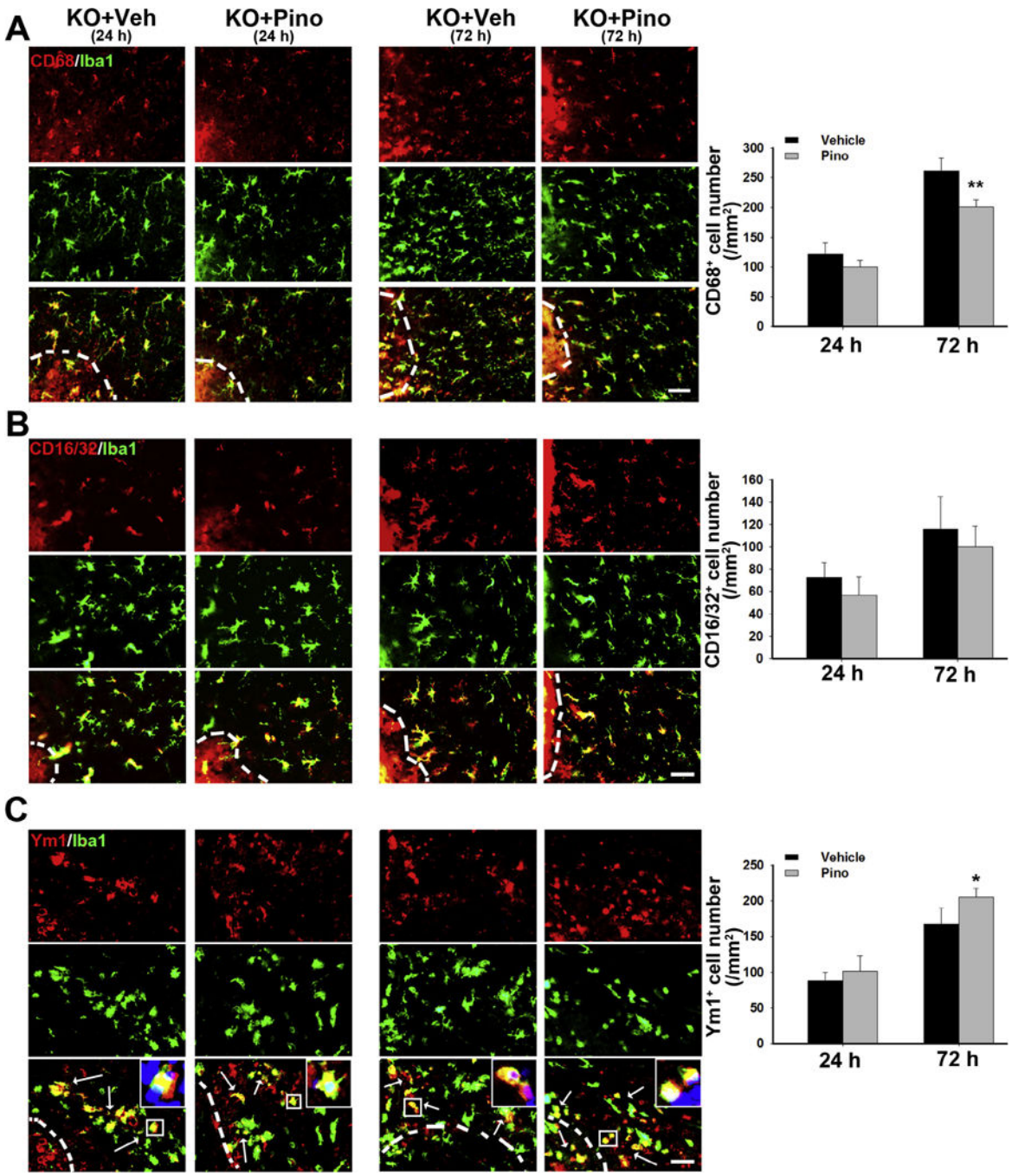

Fig. 5.

Pinocembrin decreases microglial activation and increases M2 phenotype microglia but does not decrease M1 phenotype microglia in TLR4$^{lps\text{-}del}$ (KO) mice. (A) Immunostaining of CD68 (red) and Iba1 (green) to show microglial activation. (B) Immunostaining of CD16/32 (red) and Ib1 (green) to show M1 phenotype microglia. (C) Immunostaining of YM-1 (red), Iba1 (green), and DAPI (blue) to show M2 phenotype microglia. The insets represent higher magnification of the boxed area in the corresponding merged images. White lines in A-C indicate the border of the hematoma. n = 6 mice/group; *$p < 0.05$, **$p < 0.01$ *vs.* vehicle

group. Scale bar = 40 μm. All data are presented as mean ± S.D. (For interpretation of the references to color in this figure legend, the reader is referred to the web version of this article.)

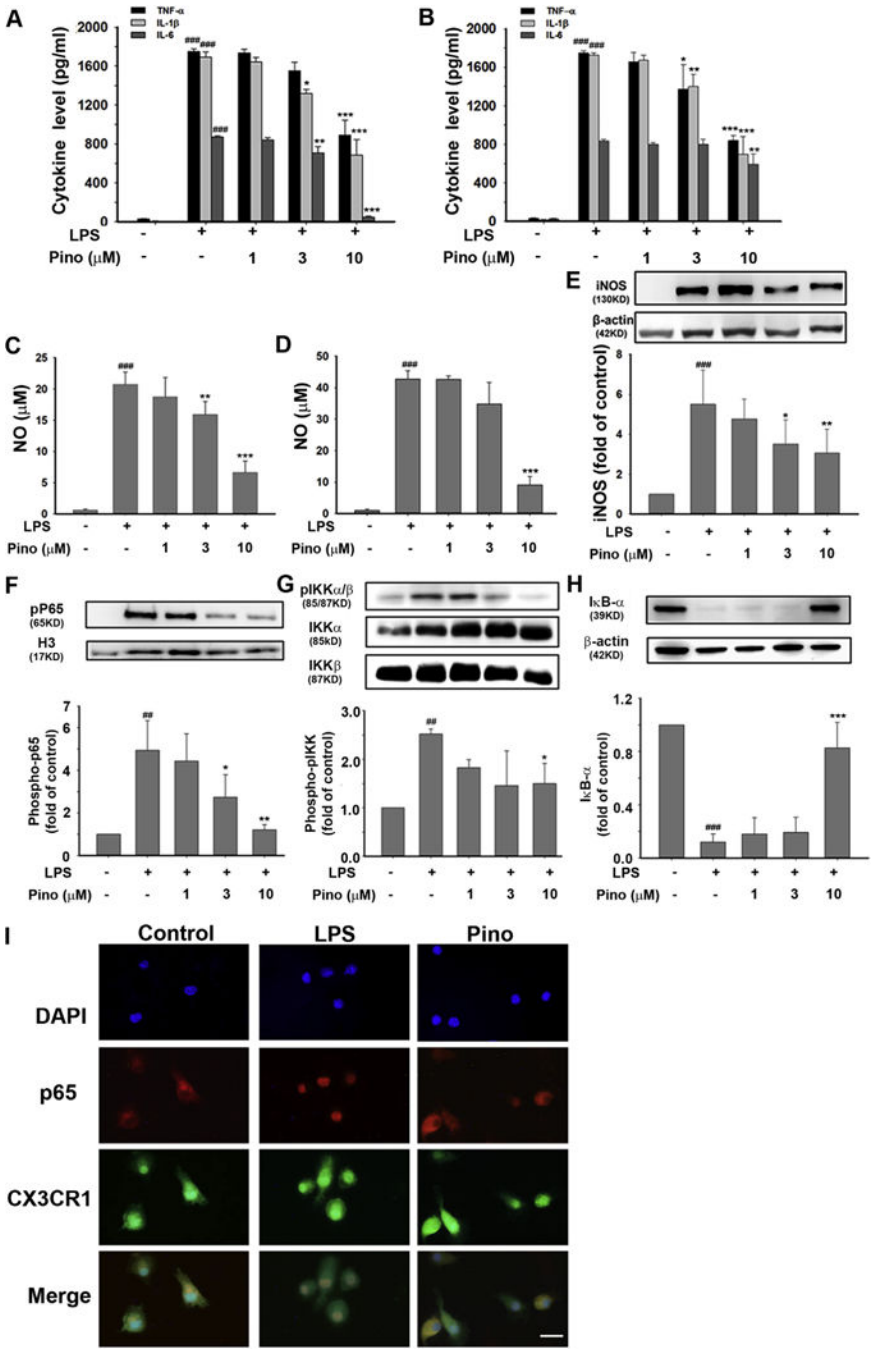

Fig. 6.

Pinocembrin decreases proinflammatory mediators released from LPS-stimulated microglia. Pinocembrin (1, 3, or 10 μM) was added to BV-2 cells (A, C, E, F, G, H) or primary microglia (B, D, I) 1 h before they were stimulated with LPS (50 ng/ml). (A, B) Pinocembrin dose-dependently inhibited the secretion of proinflammatory cytokines TNF-α, IL-1β, and IL-6 in LPS-stimulated BV-2 cells (A) and primary microglia (B). (C, D) Pinocembrin decreased the production of NO in the BV-2 cells (C) and primary microglia (D). (E) Pinocembrin dose-dependently reduced the expression of iNOS in LPS-stimulated

BV-2 cells. (F, G, H) Pinocembrin decreased the phosphorylation of nuclear p65 (pP65, F) and the phosphorylation of IKKα/β (pIKK, G), and increased the expression of IκB-α (H) in LPS-stimulated BV-2 cells. (I) Pinocembrin reduced p65 (red) transcript in the microglial (GFP) nucleus (DAPI). Scale bar = 10 μm. All data are presented as mean ± S.D. of five independent experiments. $^{###}p < 0.001$ *vs.* control group; $^{*}p < 0.05$, $^{**}p < 0.01$, $^{***}p < 0.001$ *vs.* LPS group. (For interpretation of the references to color in this figure legend, the reader is referred to the web version of this article.)

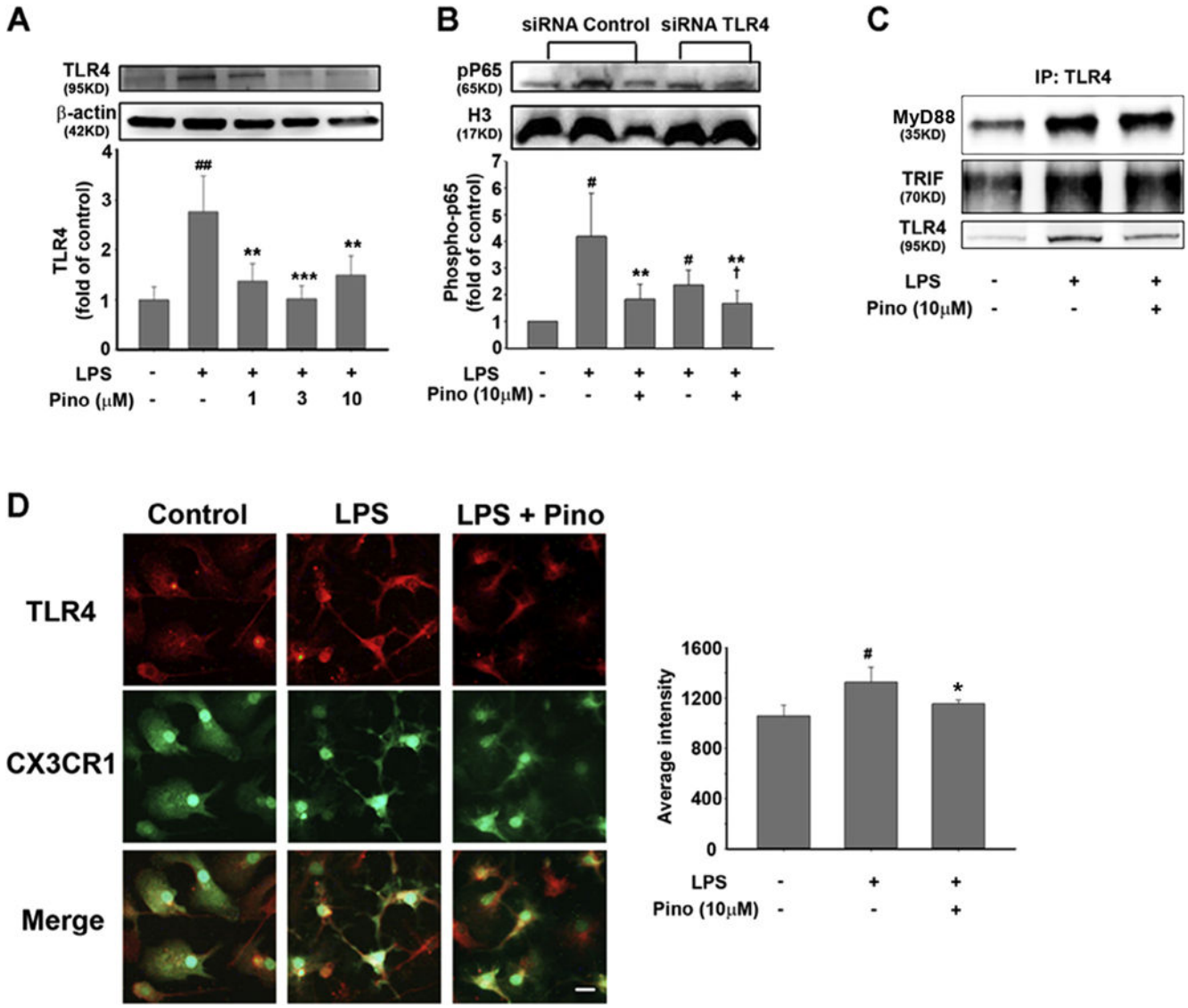

Fig. 7.

Pinocembrin reduces TLR4 expression but not TLR4/MyD88 or TLR4/TRIF interaction in LPS-stimulated microglia. (A) Expression of TLR4 in LPS (50 ng/ml)-stimulated BV-2 cells. $^{\#\#}p < 0.01$ *vs.* control group; $^{**}p < 0.01$, $^{***}p < 0.001$ *vs.* LPS group. (B) TLR4 was silenced with siRNA in BV-2 cells before 30 min of LPS stimulation. The level of phosphorylated p65 (pP65) represents the activation of NF-κB. $^{\#}p < 0.05$, $^{\#\#}p < 0.01$ *vs.* control group; $^{**}p < 0.01$ *vs.* LPS group; $^{\dagger}p < 0.05$ *vs.* siTLR4 + LPS group. (C) Immunoprecipitation was used to measure the interaction between TLR4 and MyD88/TRIF. (D) Primary microglia were stimulated by LPS for 30 min before TLR4 (red) expression was detected by immunostaining. Microglia were visualized by CX3CR1-GFP (green), and nuclei were stained with DAPI (blue). $\#p < 0.05$ *vs.* control group; $^{*}p < 0.05$ *vs.* LPS group. All data are presented as mean ± S.D. of five independent experiments. Scale bar = 10 μm. (For interpretation of the references to color in this figure legend, the reader is referred to the web version of this article.)

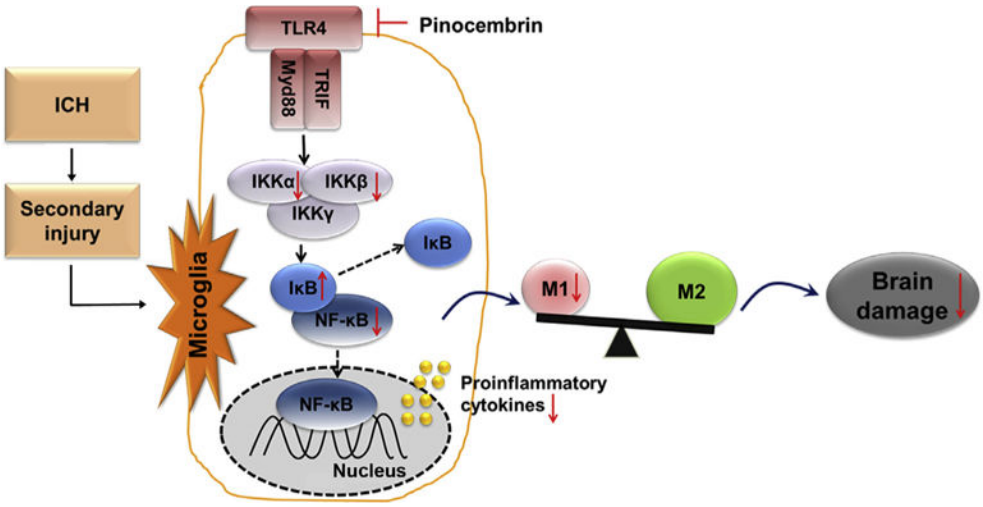

Fig. 8.

Main mechanisms of pinocembrin action after ICH. Pinocembrin reduces TLR4 expression but does not affect interactions between TLR4 and MyD88/TRIF. The TLR4 reduction leads to a decrease in phosphorylated IKK, an increase in IκB, and NF-κB inactivation, which in turn inhibits downstream inflammatory mediators, thereby inhibiting microglial M1 polarization. Our findings indicate that pinocembrin protects against ICH injury primarily by reducing M1 phenotype microglia through TLR4 signaling pathways.